Article

Advanced Science, Engineering and Medicine
Vol. 9, 1–4, 2017
www.aspbs.com/asem

Gum Mediated Synthesis and Characterization of In_2O_3 Nano Particles

Ch. Kanchana Latha[1], Y. Aparna[2,*], Ramchander Merugu[3], and P. Srinivas Subba Rao[4]

[1] *Department of Physics GDC Khairatabad, Hyderabad, Telangana, India*
[2] *Department of Physics JNTUH, CEH, Kukatpally, Hyderabad, Telangana, India*
[3] *Department of Biochemistry, Mahatma Gandhi University, Nalgonda, Telangana, India*
[4] *School of Nano Science and Technology, JNTU, Kakinada, Andhra Pradesh, India*

The yellowish Indium Oxide nanoparticles obtained from Neem gum is a new useful Biosynthesis Method using cheap precursors by a simple, cost effective and environment friendly route using Indium (III) Acetyal Acetonate. The precursor was characterized by TG-DTA to determine the crystallization temperature and thermal decomposition is found to be above 450 °C. Thermal studies of In_2O_3 confirmed complete conversion of In_2O_3 around 500 °C–600 °C. Powder X-ray diffraction (XRD) pattern of sintered In_2O_3 nano particles revealed the formation of phase pure cubic In_2O_3. The crystallite size of In_2O_3 nano particles increased from 12–25 nm. UV-visible Raman, PSA, SEM and EDX and FTIR characterization analysis showed that the In_2O_3 samples are cubic.

Keywords: Indium Oxide, Nano Particles, XRD, UV-Vis, RAMAN, SEM and EDX, PSA, FTIR, PL.

1. INTRODUCTION

As an important Transparent Conducting Metal Oxides (TCOS) with a wide band-gap of 3.55–3.75 eV, In_2O_3 has attracted considerable attention because of its high electron affinity and low electron effective mass and increasingly extensively applications in Fuel Cells,[1–4] Sensors[5] Nano Scale Transmitters[6] and Flat-Panel Display Materials.[7] In the past decade, In_2O_3 nano particles,[8–10] nano wires,[11] nano rods,[12] nano belts,[13,14] nano crystal chains,[15] nano tubes,[16,17] nano towers,[18] hollow spheres,[19,20] and micro arrows[21] have been widely emphasized to extend their technological application. Among other established Synthesis Methods, Green Synthesis Route is simple, cost effective and environmental friendly method.

Neem gum was obtained from the incised trunks of local *Azadirachta indica* (*Meliaceae*) plant. The gum was free from microbial contamination and it is rich source of protein and used as a bulking agent and for the preparation of special purpose foods namely *Escherichia coli*, *Salmonella, Pseudomonas aeruginosa, Staphylococcus awrews*. Neem gum is a potential film forming agent.[22] Here, we report for the first time the novel synthesis of In_2O_3 nano particles with particle sizes of 5–15 nm using Indium (III) Acetyl Acetonate and Neem gum mixture. Nano particles are formed after calcination the precursor of Indium Oxide in air at 500 °C–600 °C for 2 hours. This simple Green Synthesis Method in Figure 1 provides high yield nanosized materials with well crystalline structure and good photo luminescence properties.

2. EXPERIMENTAL DETAILS, GREEN SYNTHESIS TECHNIQUE

2.1. Physical Characterization

Thermal characteristics of the precursor material were studied on TG/DTA and DSC unit at a heating rate of 10 °C/min. The visible transmission was recorded on a Hitachi Spectrophotometer. The calcined powders were further characterized by particle size analysis and powder X-ray diffraction (XRD) X-ray Diffractometer (XRD) with Mono-Chromation Cuk_α Target (1.5406 Å) at a scan rate of 2°/min. Unit cell parameter was calculated from the observed '*d*'-spacing, which was accurately measured with the help of silicon as an internal standard. Cary Eclipse Spectrophotometer employing 15 W Xe flash lamp was used for the photo luminescence studies. The transmittances and band gaps were measured using an UV

*Author to whom correspondence should be addressed.

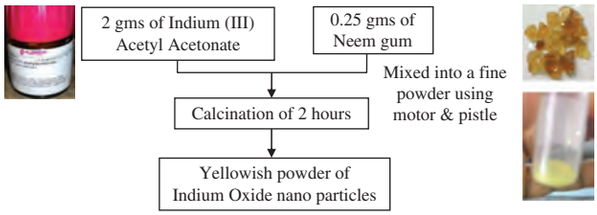

Figure 1. Flow chart of preparation of In_2O_3 nanoparticles.

visible spectrometer, FTIR and RAMAN SPECTRA are also studied.

3. RESULTS AND DISCUSSION

3.1. TGA and DTA Analysis

In Figure 2 there is an endothermic peak at 105.51 °C corresponding to the evaporation of OH. There is an endothermic peak at 191.8 °C too. This is due to the existence of organic solvent CO, OH desorption. The exothermic peak at 201.38 °C is heat release by decomposition of organic substance. There is an endothermic peak at 461.47 °C corresponding to decomposition of Indium and Neem gum and heat absorbing action. The amorphous phases changed into cubic crystal structure cause exothermic peaks at 601.98 °C and 687.31 °C. Because no impurity is introduced in the experimental process, Neem gum is considered to enter into In_2O_3 crystal lattice. The final mass loss per cent is 24% in the TGA graph. Indium Oxide nano powder is obtained by sintering the precursor at 500 °C for 2 hours.

3.2. X-ray Diffraction Studies

XRD measurements showed a cubic bixbyite structure of Indium Oxide. The angles at which the peak intensifies occur in Figure 3 is related to the inter-planar distances of the atomic structure of Indium Oxide according to Bragg's law: $n\lambda = 2d \sin\theta$, where λ is the wave length of X-ray radiation used, θ is the peak position angle and d is the inter-planar distance ($a = 10.22$ Å) but exhibit a slight decrease in the lattice constant ($a = 10.208$ Å), which was found to be in agreement with the literature.[23] The average grain sizes of the powders were calculated with the Scherer Equation, $D = 0.9\lambda/\beta\cos\theta$ where λ is the X-ray wave length (0.15406 nm), β is the Full Width at Half-Maximum intensity (FWHM) of the diffraction line, and θ is the Bragg angle. The average grain size was found to be 16.5 nm and the lattice parameter was calculated.

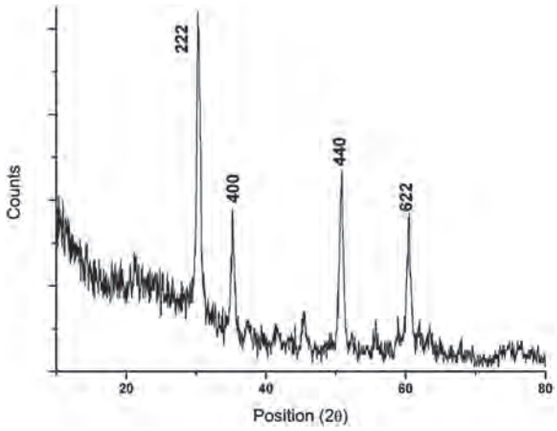

Figure 3. XRD patterns of nanocrystalline In_2O_3 samples calcined in air for 2 hours.

3.3. RAMAN Studies

The peaks in Figure 4 are observed in the Raman spectra in the range 400–2000 cm^{-1} are due to C–H bendings. Similar observations are made in FTIR spectra which indicate the presence of Neem gum extract layer on the surface of In_2O_3 nano particles. Thus Raman spectra of In_2O_3 stabilised by neem gum reflect the conformational similarities of FTIR of same samples most clearly in the lower frequency range.

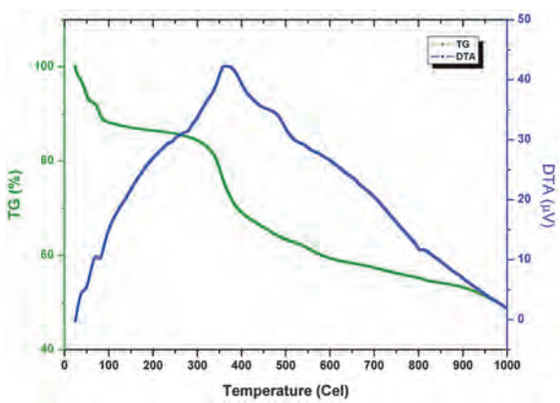

Figure 2. TG-DTA curves of thermal decomposition of In_2O_3 precursor at a heating rate of 10 °C/min in static air.

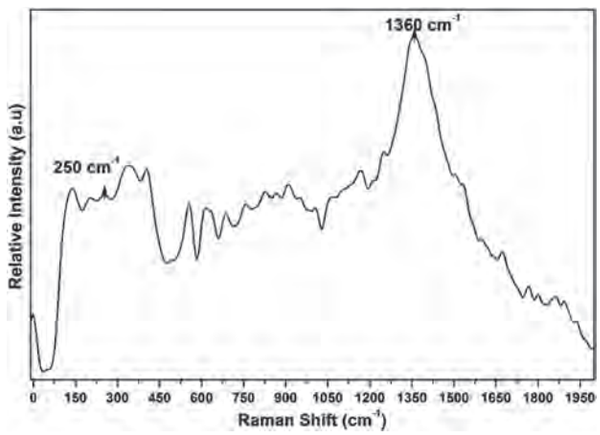

Figure 4. Raman spectra of the In_2O_3 nanoparticles stabilised by neem gum.

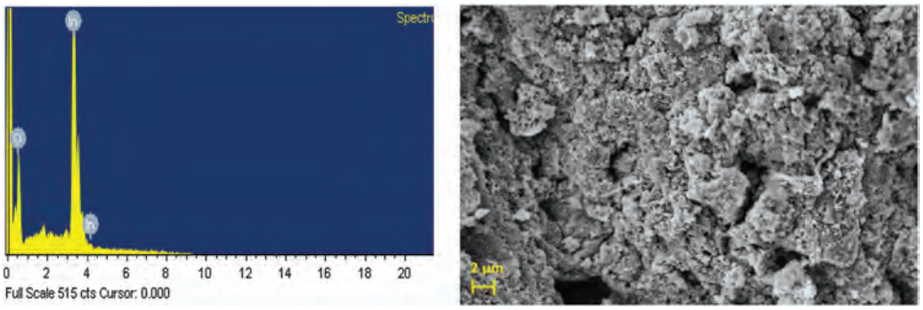

Figure 5. EDAX and SEM of In_2O_3 nano particles.

3.4. SEM and EDAX Studies

Figure 5 shows the EDAX and SEM image of as prepared In_2O_3 nano particles stabilised by neem gum extract. The nano particles obtained in this method show the nearly spherical along with the poly dispersed distribution of particle sizes. But the degree of poly dispersity is observed to be small. In the SEM image the agglomeration of In_2O_3 nano particles is well controlled because of the usage of stabilised neem gum effectively which prevent the In_2O_3 nano particles from agglomeration and also from oxidation. It can be concluded that the neem gum plays an important role in controlling the size of the prepared In_2O_3 nano particles. The EDAX pattern of In_2O_3 nano particles prepared are displayed in Figure 5. Signals of O atoms along with the strong signals of In atoms. The sample obtained from neem gum confirms the presence of In_2O_3 phase and their chemical composition is found to be 2:3 which is in good agreement. The weight and atomic percentage of Oxygen and Indium are (20.2 and 79.8) and (64.5 and 35.5) respectively.

3.5. UV-Vis Absorbance

The absorption against wave length curves recorded as shown in Figure 6. It is noticed that the reaction is very fast initially and then becomes slow because of the capping action of the proteins present in Neem gum extract. A single strong peak with a maximum around 239.6 nm is observed with gradual increase in its intensity. The Neem gum containing amino acids, proteins and poly saccharides are responsible for the stabilization of In_2O_3 nano particles. There are no other peaks located indicating the absence of nano particle aggregation.

3.6. PSA

From particle size analyzer (PSA) in Figure 7, the particle size is found to be 20 nm which is in agreement with the XRD data.

3.7. FTIR Spectra of In_2O_3 Nano Particles

The FTIR spectra of In_2O_3 sample is shown in Figure 8. The broad and strong bands are observed in these spectra at around 3455 cm^{-1} and 1594 cm^{-1} corresponding to O–H stretching frequency along with bands observed at around 1480 cm^{-1} and 1490 cm^{-1} corresponding C–H stretching.[24] The absorption peaks that appeared at around 1480 cm^{-1} and 1490 cm^{-1} are due to O–H bending. It is clear from the figure that the peaks in the range 650–1000 cm^{-1} of natural extracts are shifted slightly to higher wave numbers when compared with the FTIR

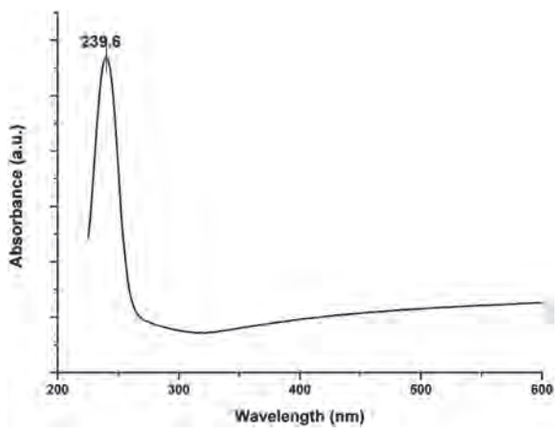

Figure 6. Room temperature optical absorbance spectra of nanocrystalline In_2O_3 samples calcined in air for 2 hours.

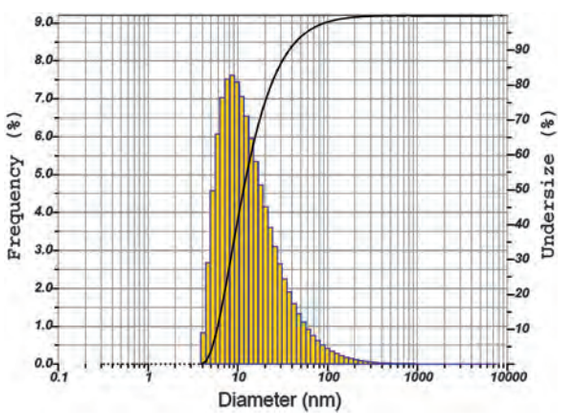

S.P. Area Ratio	Mean	S.D.	Mode
1.00	20.3 nm	48.5 nm	8.6 nm

Figure 7. PSA of In_2O_3 nano particles.

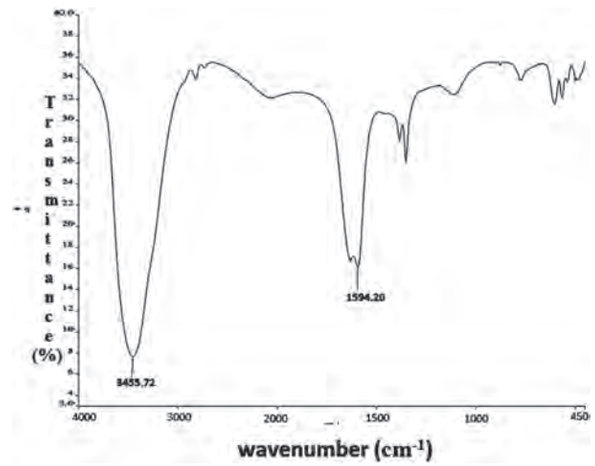

Figure 8. FTIR spectra of In_2O_3 nano particles cm^{-1}.

spectra of natural extract stabilized In_2O_3 nano particles. These differences indicate that the thin layer of natural extract molecule is developed on the surface of In_2O_3 nano particles.

3.8. PL Spectrum

PL spectrum of In_2O_3 nano crystals seems to be independent of the particle size but the synthesis route PL (optical studies): the optical properties of the In_2O_3 nano particles were analysed with PL Spectroscopy. The PL Spectra excitation in Figure 9 is at 373 nm and the band gap value is given by 3.32 eV. The observed red shift of the peak confirmed the results of In_2O_3 particles which are in nano size. The optical band gap of the nano crystalline particles depends on the particle radius due to quantum confinement.[25]

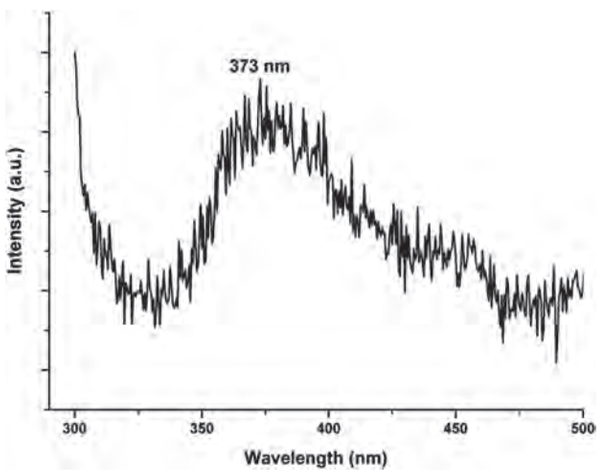

Figure 9. PL of In_2O_3 nanoparticles.

4. CONCLUSION

Structural, optical and thermal properties of In_2O_3 powders with 16 nm in grain size which annealed in a furnace of 2 hour at a temperature range of 500 °C in air atmosphere were studied. XRD results showed that the crystallinity of In_2O_3 powder was improved with annealing less than 25 nm in grain size obtained at 500 °C, which slowly increases with respect to temperature rise. The allowed direct band gap energies were calculated in good agreement. Further from the results we may conclude that the annealing temperature plays a major role in controlling the optical transmittance of the nano particle.

References and Notes

1. J. Parrondo, R. Santhanam, F. Mijangos, and B. Rambabu, *Int. J. Electrochem. Sci.* 5, 1342 (**2010**).
2. A. O. Neto, R. W. R. Verjulio-Silva, M. Linardi, and E. V. Spinace, *Int. J. Electrochem. Sci.* 4, 954 (**2009**).
3. J. Arun Kumar, P. Kalyani, and R. Saravanan, *Int. J. Electrochem. Sci.* 3, 961 (**2008**).
4. B. Krishnamurthy and S. Deepalochani, *Int. J. Electrochem. Sci.* 4, 386 (**2009**).
5. D. Zhang, Z. Liu, C. Li, T. Tang, X. Liu, S. Han, B. Lei, and C. Zhou, *Nano Lett.* 4, 1919 (**2004**).
6. P. Nguyen, H. T. Ng, T. Yamada, M. K. Smith, J. Li, J. Han, and M. Meyyappan, *Nano Lett.* 4, 651 (**2004**).
7. J. Cui, A. Wang, N. L. Edleman, J. Ni, P. Lee, N. Armstrong, and T. J. Marks, *Adv. Mater.* 13, 1476 (**2001**).
8. Q. Tang, W. Zhou, W. Zhang, S. Qu, K. Jiang, W. Yu, and Y. Qian, *Cryst. Growth and Des.* 5, 147.
9. C. Lee, M. Kim, T. Kim, A. Kim, J. Paek, J. Lee, S. Choi, K. Kim, J. Park, and K. J. Lee, *Am. Chem. Soc.* 128, 9326 (**2006**).
10. Q. Liu, W. Lu, A. Ma, J. Tang, J. Lin, and J. Y. Fang, *J. Am. Chem. Soc.* 127, 5276 (**2005**).
11. C. Liang, G. Meng, Y. Lei, F. Phillipp, and L. Zhang, *Adv. Mater.* 13, 1330 (**2001**).
12. J. Yang, C. Lin, Z. Wang, and J. Li, *Inorg. Chem.* 45, 8973 (**2006**).
13. J. Jeong, J. Lee, C. Lee, S. An, and G. Yi, *Chem. Phys. Lett.* 384, 246 (**2004**).
14. Z. Pan, Z. Dai, and Z. Wang, *Science* 291, 1947 (**2001**).
15. J. Lao, J. Huang, D. Wang, and Z. Ren, *Adv. Mater.* 16, 65 (**2004**).
16. C. Chen, D. Chen, X. Jiao, and C. Wang, *Chem. Commun.* 4632 (**2006**).
17. Y. Li, Y. Bando, and D. Golberg, *Adv. Mater.* 15, 581 (**2003**).
18. Y. Yan, Y. Zhang, H. Zeng, and L. Zhang, *Cryst. Growth and Des.* 7, 940 (**2007**).
19. P. Zhao, T. Huang, and K. Huang, *J. Phys. Chem. C* 111, 12890 (**2007**).
20. B. Li, Y. Xie, M. Jing, G. Rong, Y. Tang, and G. Zhang, *Langmuir* 22, 9380 (**2006**).
21. D. A. Magdas, A. Cremades, and J. Piquerasb, *Appl. Phys. Lett.* 88, 113107 (**2006**).
22. A. P. Kulkarni, Y. R. Shaik, and M. H. D. Dehgham, *Inventi Rapid Pharma Tech.* 1 (**2010**).
23. A. Gupta, *Japanese Journal of Applied Physics* 43, L1592 (**2004**).
24. Jovanovic, J. Stojkovska, B. Obradovic, and V. Miskovic-Stankovi, *Mater. Chem. Phys.* 133, 182 (**2012**).
25. J. J. Urban, D. V. Talapin, E. V. Sherchenko, and C. B. Murray, 128, 3248 (**2006**).

Received: 30 November 2016. Accepted: 14 March 2017.